4

Exergoeconomic Analysis and Optimization of Solar Thermal Power Plants

Ali Baghernejad and Mahmood Yaghoubi
Mechanical Engineering School, Mechanical Engineering School, Shiraz University, Iran

1. Introduction

There is a growing demand for electricity in the developing countries. The conventional approaches to meet this need are through the construction of fossil-fuel power plants. The operation of these plants, however, releases carbon dioxide and contributes to the problem of climate change. Furthermore, many of these countries rely on imports for their energy needs and the purchase of fossil fuel weakens their financial potential. Unlike hydrocarbon energies, renewable energy can be developed from resources which are constantly replenished and will never run out. These energies include:

- Solar Power which utilizes the energy from sunlight either indirectly or directly. It can be used for heating and cooling, generating electricity, lighting, water desalination, and many other commercial and industrial uses.
- Wind Power which captures the energy of the wind through wind turbines.
- Biomass Energy which uses the energy from plants and plant-derived materials, such as wood, food crops, grassy and woody plants, residues from agriculture or forestry, and the organic component of municipal and industrial wastes.
- Geothermal Energy which utilizes the heat from the earth, drawn from hot water or steam reservoirs in the earth's mantle located near the earth's surface.
- Ocean Energy which traps thermal energy from the sun's heat and mechanical energy from the tides, underwater currents and waves.
- Hydropower which captures the energy from flowing water to power machinery and produce electricity

Many developing countries have an abundance of a natural energy source: solar radiation. Operation of solar thermal power plants (STPP) would reduce their reliance on fossil fuels. Regions that could make use of these systems include Southern Africa, Middle East and North Africa (MENA) India, Northern Mexico and parts of South America. The developed regions of Southwest U.S. and Australia could also benefit from this technology.

In this chapter attempt is made to have a brief introduction of solar thermal power plant (STPP) systems and cycles. To develop new approaches to exergoeconomic analysis of such plants, the main elements of exergy and economic analysis are explained. Various methods of optimization from single objective to multi objectives applicable to STPP are developed. Finally application of the developed optimization methods for a sample integrated solar

combined cycle system (ISCCS) are illustrated. It has been shown that the new optimization schemes are strong tools which can be used to find optimum operating condition based on the main objectives of any thermal plant.

2. Solar parabolic trough systems

Solar thermal power plants (STPP) are one of the promising options for electricity supply as demonstrated in some countries during the past decades (Singh & Kaushik, 1994). These plants with parabolic trough type of solar collectors featuring gas burners and Rankine steam cycles have been successfully demonstrated by California's Solar Electric Generating Systems (SEGS).

Trough systems use linear concentrators of parabolic shape with highly reflective surfaces, which can be turned in angular movements towards the sun position and concentrate the radiation onto a long-line receiving absorber tube. The absorbed solar energy is transferred by a working fluid, which is then piped to a conventional power conversion system. The used power conversion systems are based on two technologies:

- Rankine-Cycle STPP
- Integrated Solar Combined-Cycle Systems (ISCCS) and other hybrid systems.

Rankine-cycle plants are a mature technology that offers a high solar contribution. Recently, integrating the solar collector system with a gas-fired combined-cycle system has been proposed as a lower cost alternative for generating solar-powered electricity.

2.1 Rankine-cycle systems

The Rankine-cycle STPP is a steam-based power plant with solar energy as the heat source. The system is a typical Rankine cycle (see Figure 1). The hot collector heat transfer fluid transfers its heat in the heat exchanger to the water/steam. The steam drives the turbine to produce electricity. The spent steam is condensed into water in the condenser. The water is reheated in the heat exchanger and the cycle repeats. Because of the seasonal and daily variation in solar radiation, a Rankine-cycle system can only be expected to operate at full load for approximately 2400 hours annually (25% capacity factor) without the use of thermal storage. In most cases, it makes sense to add a fossil-fuel heater so that the system can operate at full load for more hours. Back-up fuels can be coal, oil, naphtha and natural gas. The number of hours that such plant can operates depends on the local conditions. In most cases, however, it makes sense to operate this type of plant to meet the daily periods of high demand for electricity (10 to 12 hours per day). However, Rankine-cycle systems suffer from relatively low efficiencies (whether solar or fossil-fuel powered). The conversion of heat to electricity has an efficiency of about 40%. If the conversion efficiency from fossil fuel to heat is included, the plant efficiency drops to approximately 35% (Status Report on Solar Thermal Power Plants, 1996).

2.2 Integrated solar combined cycle systems

Between 1984 and 1990, Luz International Limited developed, built, and sold nine parabolic trough solar power plants in the California Mojave Desert. These plants, called Solar Electric Generating Stations and referred to as SEGS I– IX, range in size from 14 MWe to 80 MWe and make up a total of 354 MWe of installed generating capacity. The details of these plants are summarized in Table 1 (www.greenpeace.org, 2005).

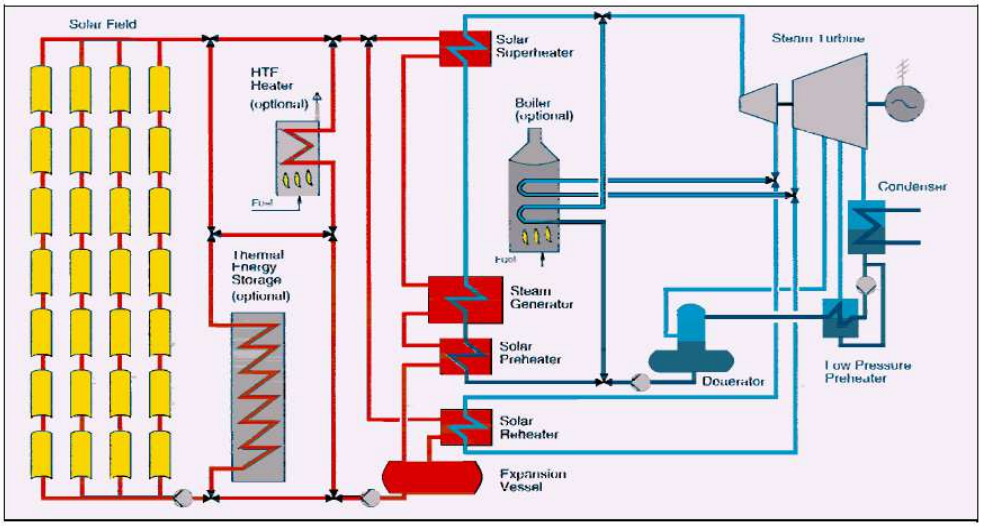

Fig. 1. Schematic diagram of a Rankine- Cycle STTP

The SEGS plants in California utilized a solar steam system to provide inlet steam for a conventional (Rankine) cycle steam turbine power plant. In addition to the standard SEGS configuration, Luz International Limited conceived a system configuration for a solar field integrated with a gas-fired combined cycle plant. This concept, known as the Integrated Solar Combined Cycle System (ISCCS), is derived from a conventional combined cycle design in which the exhaust heat from the combustion turbine generates steam in a heat recovery steam generator (HRSG) to drive a steam turbine connected to a generator, with supplemental heat input from the solar field to increase the steam to the steam turbine (Baghernejad & Yaghoubi, 2010). This approach offers a potentially more cost effective and thermodynamically efficient method to utilize solar thermal energy to produce electricity compared to the use of solar energy with a conventional boiler fired (Rankine) cycle plant. In comparison to existing Rankine cycle power plants with parabolic trough technology (SEGS), ISCCS plants offer three principal advantages: First, solar energy can be converted to electric energy at a higher efficiency. Second, the incremental costs for a larger steam turbine are less than the overall unit cost in a solar-only plant. Third, an integrated plant does not suffer from the thermal inefficiencies associated with the daily start-up and shutdown of the steam turbine. Crucial issues in the effective utilization of parabolic trough solar fields in combination with combined cycle plants are the ability to achieve a significant reduction in global emissions, the effective annual heat rate of the combined system, and the cost impact on the plant output (Baghernejad & Yaghoubi, 2011a).

Unit	I	II	III	IV	V	VI	VII	VII	IX
Capacity (MW)	13.8	30	30	30	30	30	30	80	80
Land Area (ha)	29	67	80	80	87	66	68	162	169
Solar field aperture area (ha)	8.3	19	23	23	25.1	18.8	19.4	46.4	48.4
Solar field outlet temperature (^{0}C)	307	321	349	349	349	391	391	391	391
Annual Performance (Design value)									
Solar field thermal efficiency (%)	35	43	53	53	53	53	53	53	50
Solar to net electrical efficiency (%)	9.3	10.7	10.2	10.2	10.2	12.4	12.3	14	13.6
Net electricity production (GWh/yr)	30.1	80.5	91.3	91.3	99.2	90.9	92.6	252.8	256.1
Unit cost ($/kW)	4490	3200	3600	3730	4130	3870	3870	2890	3440

Table 1. Characteristics of Luz SEGS plants (www.greenpeace.org, 2005)

3. Exergy analysis

Exergy is defined as the maximum possible reversible work obtainable in bringing the state of a system to equilibrium with that of environment (Bejan et al., 1996). The physical exergy component is associated with the work obtainable in bringing a stream of matter from its initial state to a state that is in thermal and mechanical equilibrium with the environment. The chemical exergy component is associated with the work obtainable in bringing a stream of matter from the state that is in thermal and mechanical equilibrium with the environment to a state that is in the most stable configuration in equilibrium with the environment. Therefore the exergy of any state of system is:

$$\dot{E} = \dot{E}_{PH} + \dot{E}_{CH} \tag{1}$$

The physical exergy component is calculated using the following relation:

$$\dot{E}_{PH} = \dot{m}[(h - h_0) - T_0(s - s_0)] \tag{2}$$

The exergy of the air and gas streams per unit mass are defined by (Moran & Sciubba, 1994):

$$e_i = C_{p,Air(Gas)}[T_i - T_0 - T_0 \ln(\frac{T_i}{T_0})] + R_{Air(Gas)} T_0 \ln(\frac{P_i}{P_0}) \tag{3}$$

Energy and exergy analyses for a solar collector-receiver subsystem, Fig. 2 have been carried in Baghernejad and Yaghoubi (2010).

Fig. 2. Typical solar collector-receiver subsystem

4. Economic model

The economic model takes into account the cost of the components, including amortization and maintenance, and the cost of fuel consumption. In order to define a cost function which depends on the optimization parameters of interest, component costs have to be expressed as functions of thermodynamic variables (Baghernejad & Yaghoubi, 2011a, 2011b). These relationships can be obtained by the statistical correlations between costs and the main thermodynamic parameters of the component performed on real data series. The expressions of purchase components costs and amortization factor are accepted here similar to (Schwarzenbach & Wunsch, 1989). Its format is widely used by various authors but some coefficients were adapted to quotation made by manufacturers. The new coefficients also taken into account the installation, electrical equipment, control system, piping and local assembly.

5. Exergoeconomic principles

In the analysis and design of energy systems, the techniques which combine scientific disciplines with economic disciplines to achieve optimum design are growing in the energy industries (Valero, 2004). Exergoeconomic analysis as a powerful scheme is such a method that combines exergy analysis with economic studies. This method provides a technique to evaluate the cost of inefficiencies or cost of individual process streams, including intermediate and final products of any system. These costs are applicable in feasibility studies, for investment decisions, on comparing alternative techniques and operating conditions, in a cost-effective section of equipments during an installation, and an exchange or expansion of an energy system (Johansson, 2002; Verda, 2004). Also it can be utilized in optimization of thermodynamic systems, in which the task is usually focused on minimizing the unit cost of the system product.

The prerequisite for the exergoeconomic analysis is a proper 'fuel–product–loss' (F-P-L) definition of the system to show the real production purpose of its subsystems by attributing a well defined role, i.e. fuel, product or loss, to each physical flow entering or leaving the subsystems. The fuel represents the resources needed to generate the product and it is not necessarily restricted to being an actual fuel such as natural gas, oil, and coal. The product represents the desired result produced by the system. Both the fuel and the product are expressed in terms of exergy. The losses represent the exergy loss from the system. Once the F–P–L of a system is defined according to (Baghernejad & Yaghoubi, 2011a; Lozano & Valero, 1993), appropriate cost can be allocated to the products, fuels and losses occurring in the system. A detailed exergy analysis includes calculation of exergy destruction, exergy loss, exergetic efficiency and exergy destruction ratio in each component of the system along with the overall system. Mathematically, these are expressed as follows (Tsatsaronis & Pisa, 1994):

$$\dot{E}_{D,k} = \dot{E}_{F,k} - \dot{E}_{P,k} - \dot{E}_{L,k} \tag{4}$$

$$\varepsilon = \frac{\dot{E}_P}{\dot{E}_F} = 1 - \frac{\dot{E}_D + \dot{E}_L}{\dot{E}_F} \tag{5}$$

$$\chi_k = \frac{(\dot{E}_D)_k}{(\dot{E}_D)_{Tot}} \tag{6}$$

Exergy costing involves cost balances formulated for each system component separately. A cost balance applied to the kth component shows that the sum of cost rates associated with all exiting exergy streams equals the sum of cost rates of all entering exergy streams plus the appropriate charges (cost rate) due to capital investment and operating and maintenance expenses. The sum of the last two terms is denoted by $\dot{Z}$. Accordingly, for a kth component:

$$\sum_{e}^{N}(c_e\dot{E}_e)_k + c_{w,k}\dot{W}_k = c_{q,k}\dot{E}_{q,k} + \sum_{i}^{N}(c_i\dot{E}_i)_k + \dot{Z}_k \tag{7}$$

In the above equation $\dot{Z}_k = \frac{fI_k\varphi}{H}$, where f and I_k are the annuity factor and investment cost which are calculated from those given in (Bejan et al., 1996). φ is maintenance factor and H is operation period. In general, if there are N_e exergy streams exiting the component being considered, we have N_e unknowns and only one equation, the cost balance. Therefore, we need to formulate $N_e - 1$ auxiliary equations. This is accomplished with the aid of the F and P principles in the SPECO approach (Lazzaretto & Tsatsaronis, 2006).

Developing Eq. (7) for each component of a plant along with auxiliary costing equations (according to P and F rules) leads to a system of N_e equations. By solving this system of equations, the costs of unknown streams of the system will be obtained. These are the average unit cost of fuel ($c_{f,k}$), average unit cost of product ($c_{p,k}$), cost rate of exergy destruction ($\dot{C}_{D,k}$), cost rate of exergy loss ($\dot{C}_{L,k}$), and the exergoeconomic factor (f_k). Mathematically, these are expressed as (Tsatsaronis & Pisa, 1994):

$$c_{f,k} = \dot{C}_{f,k} / \dot{E}_{f,k} \tag{8}$$

$$c_{p,k} = \dot{C}_{p,k} / \dot{E}_{p,k} \tag{9}$$

$$\dot{C}_{D,k} = c_{f,k}\dot{E}_{D,k} \tag{10}$$

$$\dot{C}_{L,k} = c_{f,k}\dot{E}_{L,k} \tag{11}$$

$$f_k = \frac{\dot{Z}_k}{\dot{Z}_k + \dot{C}_{D,k} + \dot{C}_{L,k}} \tag{12}$$

6. Optimization problem

A function optimization problem may be of different types, depending on the desired goal of the optimization task. The optimization problem may have only one objective function (known as a single-objective optimization problem), or it may have multiple conflicting objective functions (known as a multi-objective optimization problem). Some problems may have only one local optimum, thereby requiring the task of finding the sole optimum of the function. Other problems may contain more than one local optima in the search space, thereby requiring the task of finding multiple such locally optimal solutions.

Mathematically, a multi-objective optimization problem (Rao, 1996) having m objectives and n decision variables requires the minimization of the components of the vector $F(x)=\mathrm{F}(f_1(x),f_2(x),\ldots,f_\mathrm{m}(x))$, where F is the evaluation function that maps the points of the decision variable space, such as $x=\mathrm{x}(x_1,\ldots,x_\mathrm{n})$, to the points of the objective function space.

$$\begin{aligned} &\textit{Minimize} \quad (f_1(x), f_2(x), \ldots, f_m(x)) \\ &\textit{Subject to} \quad g_j(x) \geq 0, \quad j = 1,2,\ldots,J \\ &\qquad\qquad h_k(x) = 0, \quad k = 1,2,\ldots,K \\ &\qquad\qquad x_i^{(L)} \leq x_i \leq x_i^{(U)}, \quad i = 1,2,\ldots,n \end{aligned} \tag{13}$$

A multi-objective optimization problem requires the simultaneous satisfaction of a number of different and often conflicting objectives. These objectives are characterized by distinct measures of performance that may be (in) dependent and/or incommensurable. A global optimal solution to a multi-objective optimization problem is unlikely to exist: this means that there is no combination of decision variables values that minimizes all the components of vector F simultaneously. Multi-objective optimization problems generally show a possibly uncountable set of solutions, whose evaluated vectors represent the best possible trade-offs in the objective function space. The Pareto approach to multi-objective optimization (Pareto, 1896) is the key concept to establish optimal set of design variables, since the concepts of Pareto dominance and optimality are straightforward tools for determining the best trade-off solutions among conflicting objectives. An evolutionary algorithm is then chosen to carry out the search for the Pareto optimal solution because evolutionary optimization techniques already deal with a set of solutions (a population) to pursue their task, so a multi-objective Pareto-based evolutionary algorithm is able to make the population converge to the entire set of optimal solutions in a single run.

7. Evolutionary algorithms for optimization

The evolutionary algorithm is a method for solving both constrained and unconstrained optimization problems that is based on natural selection, the process that drives biological evolution (Rezende et al., 2008). As a first step, parent selection is performed with each individual having the same probability of being chosen. Suppose N_P is the size of generated population. Then N_P numbers of parents enter the reproduction step, generating N_P offspring through a crossover strategy in which the decision variable values of the offspring fall in a range defined by the decision variable values of the parents. Some of the offspring are also produced by adding a Gaussian random variable (N) with zero mean and a standard deviation proportional to the scaled cost value of the parent trial solution, i.e,

$$P'_{g,i} = P_{g,i} + N(0,\sigma_i^2) \tag{14}$$

The standard deviation σ_i indicates the range over which the offspring is created around the parent trial solution and is given by

$$\sigma_i^2 = \varphi \frac{f(\overline{P}_i)}{f(\overline{P}_{\min})} \tag{15}$$

Where $f(\overline{P}_{\min})$ is the minimum value of the objective function among the N_P trial solution, $f(\overline{P}_i)$ is the objective function value associated with the trial vector $\overline{P}_i$ and φ is a scaling factor. These offspring $\overline{P}_i'$, $i = 1,2,...,N_P$ and their parents $\overline{P}_i$, $i = 1,2,...,N_P$ form a set of $2N_P$ trial solutions and they contend for survival with each other within the competing pool. After competition, the $2N_P$ trial solutions including the parents and the offspring are ranked in descending order of the score. The first N_P trial solutions survive and are transcribed along with their objective functions $f(\overline{P}_i)$ into the survivor set as the basis of the next generation. Finally, the number of generations elapsed is compared to the established maximum number of generations. If the termination condition is met, the process stops, otherwise the surviving solutions become the starting population for the next generation (Beghi et al., 2011).

8. Exergoeconomic optimization

8.1 Single objective exergoeconomic optimization

In general, a thermal system requires two conflicting objectives: one being increase in exergetic efficiency and the other is decrease in product cost, to be satisfied simultaneously. The first objective is governed by thermodynamic requirements and the second by economic constraints. Therefore, objective function should be defined in such a way that the optimization satisfies both requirements. For a single objective optimization, the optimization problem should be formulated as a minimization or maximization problem. The exergoeconomic analysis gives a clear picture about the costs related to the exergy destruction, exergy losses, etc. Thus, the objective function in this optimization becomes a minimization

problem. Using of this technique for optimizing district heating network-using genetic algorithm (GA) demonstrated by (Cammarata et al., 1998). The objective function for this problem is defined as to minimize the total cost function $\dot{C}_{sys}$, which can be modeled as:

$$\dot{C}_{sys} = \sum_k \dot{Z}_k + \sum_k \dot{C}_{D,k} + \dot{C}_{L,k} \tag{16}$$

8.2 Multi objective exergoeconomic optimization

The two objective functions of this multi-criteria optimization problem are the total exergetic efficiency of the plant (to be maximized) and the total cost rate of product (to be minimized). The mathematical formulation of objective functions is as following (Baghernejad & Yaghoubi, 2011b):

$$\varepsilon_{Tot} = \frac{\dot{E}_W}{\dot{E}_F} \tag{17}$$

$$\dot{C}_{Tot} = \sum_k \dot{Z}_k \tag{18}$$

9. Sensitivity analysis

Sensitivity analysis is a general concept which aims to quantify the variations of an output parameter of a system regarding to the changes imposed on some input important parameters. A comprehensive sensitivity analysis can be performed to examine the impact of the variation of important factors on electricity costs of any STPP. The most important factors which influence electricity cost of a solar thermal power plant are fuel specific cost, interest rate, plant lifetime, solar field operation period and construction period (Baghernejad & Yaghoubi, 2011a, 2011b).

10. Example of application

10.1 Integrated solar combined cycle system (ISCCS)

Fig. 3 shows a schematic diagram of an integrated solar combined cycle system. This power plant contains two 125 MW gas turbines, a 150 MW steam turbine, and a 17 MW solar plant.

In this system a combined cycle unit with the following equipments is used:

- Two V94.2 gas turbine units with natural gas fuel
- Two heat recovery steam generators with two pressure lines. The high and low pressure steam conditions are: 84.8 bar and 506 ^{0}C and 9.1 bar and 231.6 ^{0}C respectively. A design stack temperature of 113 ^{0}C is selected to recover as much energy from the turbine exhaust as possible
- A no reheat two pressure steam turbine

The solar field considered in this site is comprised of 42 loops and for each loop, 6 collectors from type of LS-3 (Kearney, 1999) which are single axis tracking and aligned on a north–south line, thus tracking the sun from east to west. Various design parameters of these

collectors are given in Table 2. In this study, numerical results are based on site design condition with ambient temperature of 19 °C and a relative humidity of 32 percent and wind speed of 3 m/s. The analysis is carried out on 21 Jun at 12:00 noon (LAT). At this hour, solar radiation intensity at the plant site is about 800 W/m². Also, Therminol VP-1 is used as heat transfer fluid (HTF) in the solar field. The state properties and exergies calculated for the system of Fig.3 are given in Table 3. In this table, states 0, 0' and 0'' are the dead states for air, water and oil, respectively. In this model, the variables selected for the optimization are (Baghernejad & Yaghoubi, 2011a, 2011b):

The compressor pressure ratio $P_r (= \frac{P_2}{P_1})$, isentropic efficiency of the compressor η_{AC}, temperature of the combustion products entering the turbine T_3, isentropic efficiency of the gas turbine η_{GT} in the gas cycle, isentropic efficiency of the oil pump η_{OILP}, and oil outlet temperature in the collectors T_{28} in the solar field, temperature and pressure of the steams leaving the heat recovery steam generator T_{23}, $P_{23,17}$, isentropic efficiency of the condensed extraction pump η_{CEP} and isentropic efficiency of the boiler feed water pump η_{BFP} in the steam cycle. This model is treated as the base case and the following nominal values of the decision variables are selected based on the operation program of the constructed site. $P_r = 11$, $\eta_{AC} = 0.85$, $T_3 = 1404.8\ K$, $\eta_{GT} = 0.875$, $\eta_{OILP} = 0.8$, $T28 = 666.5 K$, $T_{23} = 779.15\ K$, $P_{23} = 84.8\ bar$, $P_{17} = 9.1\ bar$, $\eta_{ST} = 0.85$, $\eta_{CEP} = 0.8$, $\eta_{BFP} = 0.8$

10.2 Exergoeconomic analysis

The system used in Fig. 3 consists of 16 components and has 38 streams (32 for mass and 6 for work). Therefore 22 boundary conditions and auxiliary equations are necessary. For example in this system, for steam turbine (ST) and solar heat exchanger (SHE), cost balance and auxiliary costing equations (according to P and F rules) are formulated as follow:

Steam turbine:

$$\dot{C}_{11} + \dot{C}_{38} = 2(\dot{C}_{17} + \dot{C}_{23}) + \dot{Z}_{ST} \tag{19}$$

$$c_{17} + c_{23} = c_{11} \quad or \quad \frac{\dot{C}_{17} + \dot{C}_{23}}{\dot{E}_{17} + \dot{E}_{23}} = \frac{\dot{C}_{11}}{\dot{E}_{11}} \tag{20}$$

Solar heat exchanger:

$$\dot{C}_{25} + \dot{C}_{26} = \dot{C}_{24} + \dot{C}_{28} + \dot{Z}_{SHE} \tag{21}$$

$$c_{26} = c_{28} \quad or \quad \frac{\dot{C}_{26}}{\dot{E}_{26}} = \frac{\dot{C}_{28}}{\dot{E}_{28}} \tag{22}$$

In the same way developing cost balance equation for other element of oil, gas and steam cycles along with auxiliary costing equations leads to a system of equations. By solving the system of 38 equations and 38 unknowns, the cost of unknown streams of the system will be obtained. More details of cost balance equations can be seen in (Baghernejad & Yaghoubi, 2011a, 2011b).

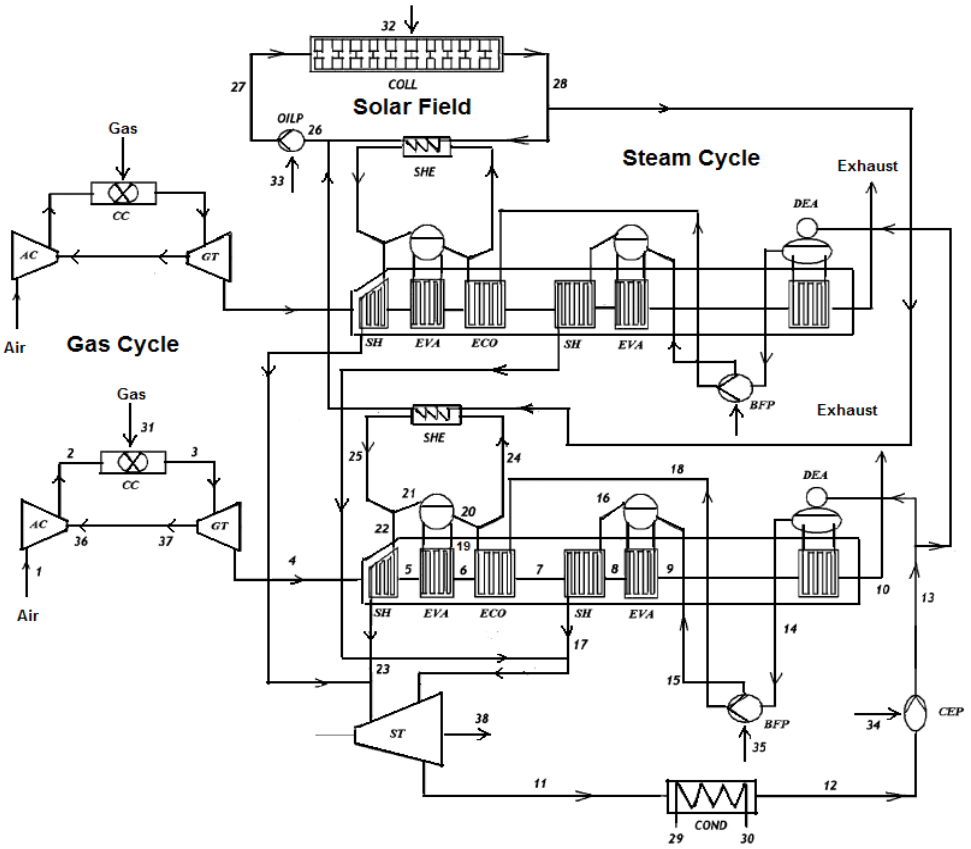

Fig. 3. Schematic diagram of a Integrated Solar Combined Cycle System

Aperture Area per SCA (m^2)	545	HCE Transmittance	0.96
Mirror Segments	224	Mirror Reflectivity	0.94
Aperture (m)	5.76	Length	99
HCE Diameter (m)	0.07	Concentration Ratio	82
Average Focal Distance (m)	0.94	Peak Collector Efficiency (%)	68
HCE Absorptivity	0.96	Annual Thermal Efficiency (%)	53
HCE Emittance	0.17	Optical Efficiency (%)	80

Table 2. LS-3 Collector specifications (Kearney, 1999)

State	$\dot{m}$ (kg/sec)	T (K)	P (bar)	h (kJ/kg)	$\dot{E}$ (MW)
0	-	292.15	1.013	292.43	-
0'	-	292.15	1.013	79.82	-
0''	-	292.15	1.013	12	-
1	421.81	292.15	1.013	292.43	0
2	421.81	630.35	11.14	631.8	132.86
3	429.56	1404.80	10.58	1409	388.29
4	429.56	821.46	1.05	823.6	105.8
5	429.56	729.67	1.07	468.15	80.24
6	429.56	536.86	1.04	261.64	31.75
7	429.56	479.67	1.04	200.65	20.59
8	429.56	477.12	1.02	197.92	19.39
9	429.56	431.1	1.02	148.67	11.87
10	429.56	386.15	1.013	100.58	6
11	144.32	321.19	0.112	2304.5	28.25
12	144.32	321.19	0.112	201.15	0.80
13	144.32	321.55	25.5	204.36	1.09
14	72.16	390.02	1.8	490.52	4.09
15	9.25	390.15	9.3	491.52	0.53
16	9.25	449.9	9.3	2774.3	7.82
17	9.25	504.74	9.1	2906	8.27
18	62.91	391.71	119	506	4.39
19	62.91	488.15	118	923.8	13.17
20	53.66	488.15	118	923.8	10.22
21	53.66	578.66	92.77	2738.2	53.1
22	62.91	578.66	92.77	2738.2	68.38
23	62.91	779.15	84.8	3408.6	91.22
24	14.06	488.15	118	923.8	2.94
25	14.06	578.66	92.77	2738.2	15.28
26	218.42	571.15	11	550.34	36.54
27	218.42	573.82	16	552.63	36.83
28	218.42	666.5	26	790	73.16
29	2575	292.15	1.013	79.82	0
30	2575	320.35	1.013	197.71	13.77
31	7.75	292.15	20	292.43	401.89

Table 3. State properties and calculated exergy of the system corresponding to Fig. 3

10.3 Result and discussion

Although the decision variables may be varied in optimization procedure, each decision variable is normally required to be within a given practical range of operation as follow (Baghernejad & Yaghoubi, 2011a):

$9 \le P_r \le 16 \quad 640 \le T_{28} \le 670\ K \quad 80 \le P_{23} \le 100\ \ bar \quad 1350 \le T_3 \le 1500\ K \quad 7 \le P_{17} \le 10\ \ bar$

$0.75 \le \eta_{AC} \le 0.9 \quad 0.75 \le \eta_{BFP} \le 0.9 \quad 0.75 \le \eta_{ST} \le 0.9 \quad 0.75 \le \eta_{GT} \le 0.9 \quad 0.75 \le \eta_{CEP} \le 0.9$

$723.15 \le T_{23} \le 823.15\ K \quad 0.75 \le \eta_{OILP} \le 0.9$

Also, the values of the economic parameters and fixed parameters for the optimization of system are given in Table 4 (Baghernejad & Yaghoubi, 2011a).

η_{CC}	0.99	LHV (kJ/kg)	47966
φ	1.06	ri (%)	8
in (%)	10	CP (year)	3
k (years)	25	$\dot{W}_{out}(MW)$	400
H (hour) for solar field	2000	H (hour) for Combined cycle	7500

Table 4. Fixed parameters for the system shown in Fig. 3 (Baghernejad & Yaghoubi, 2011a)

For a single objective optimization, with the objective function indicated in Eq. (16) in the first generation, 100 vectors $\overline{P}_i = [P_r, \eta_{AC}, T_3, \eta_{GT}, \eta_{OILP}, T_{28}, T_{23}, P_{23}, P_{17}, \eta_{ST}, \eta_{CEP}, \eta_{BFP}]$ are randomly generated within the operating range. For each trial, the objective function is evaluated through exergy analysis and exergoeconomic formulations after passing through the system constraints. Performance of the system with each vector is evaluated. The vector having the best system performance is stored for future comparison. The algorithm selects a group of vectors in the current generation, called parents that have better objective function values for the next generation (second generation). These parents are modified using Eq. (14) to generate the offsprings. The performance of the offsprings and the parent vectors are compared to select the best vector in the generation. The process of selecting parents and then generating the offsprings repeats till the specified number of generations.

The structure of the multi objective evolutionary algorithm (MOEA) used in the present work is illustrated in (Schwefwl, 1995). Also, the tuning of MOEA is performed according to the values indicated in Table 5 (Baghernejad & Yaghoubi, 2011b). Fig. 4 presents the Pareto optimum solutions for the integrated solar combined cycle system with the objective function indicated in Eqs. (17) and (18). As shown in this figure, while the total exergetic efficiency of the plant is increased to about 44%, the total cost rate of products increases very slightly. Increasing the total exergetic efficiency from 44% to 47% corresponds to the moderate increase in the cost rate of product. Further increasing of exergetic efficiency from 47% to the higher value leads to a drastic increasing of the total cost rate.

In multi-objective optimization, a process of decision-making for selection of the final optimal solution from the available solutions is required. The process of decision-making is usually performed with the aid of a hypothetical point in Fig. 5 named as equilibrium point that both objectives have their optimal values independent to the other objective. It

is clear that it is impossible to have both objectives at their optimum point, simultaneously and as shown in Fig. 5, the equilibrium point is not a solution located on the Pareto frontier. The closest point of Pareto frontier to the equilibrium point might be considered as a desirable final solution. In selection of the final optimum point, it is desired to achieve the better magnitude for each objective than its initial value of the base case problem. On the other hand, the stability of the selected point when one of objective varies is highly important. Therefore a part of Pareto frontier is selected in Fig. 6 for decision-making and coincided with domain between horizontal and vertical lines. A final optimum solution with 45.19% exergetic efficiency and the total cost rate of product equal to 10920.43 $/h as indicated in Fig. 6 is selected. It should be noted that the selection of an optimum solution depends on the preferences and criteria of each decision-maker. Therefore, each decision-maker may select a different point as optimum solution to better suits with his/her desires.

Turning parameters	Value
Population size	100
Maximum number of generations	100
P_c (probability of crossover) (%)	50
P_m (probability of mutation) (%)	1
Selection process	Tournament
Tournament size	2

Table 5. The turning parameters in MOEA optimization program (Baghernejad & Yaghoubi, 2011b)

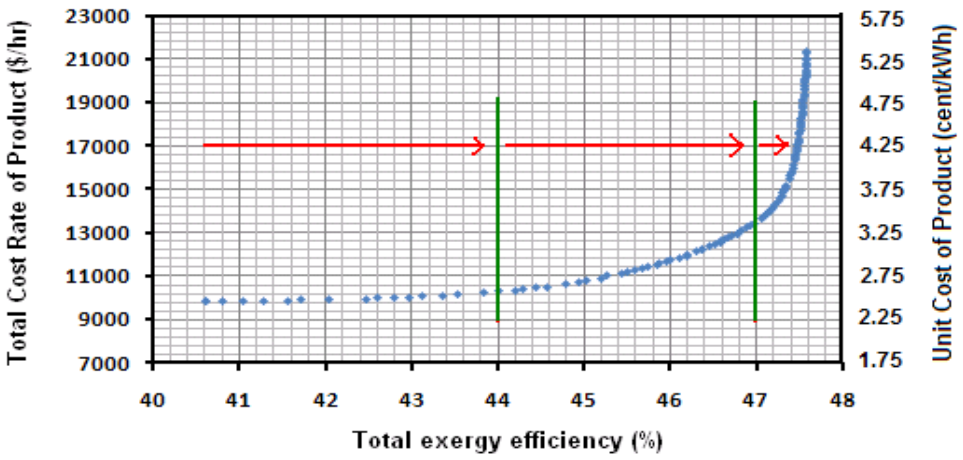

Fig. 4. Pareto optimal solutions for solar combined cycle system shown in Fig. 3

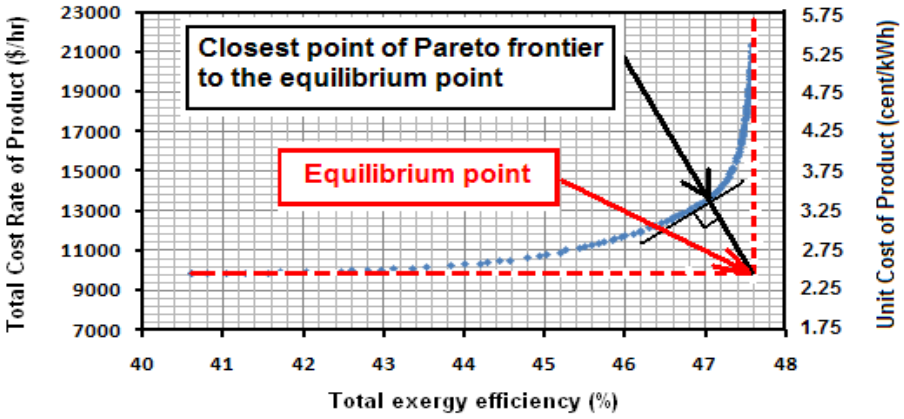

Fig. 5. Pareto frontier: best trade-off values for the objective functions (total exergetic efficiency and total cost rate of products) in the system shown in Fig. 3

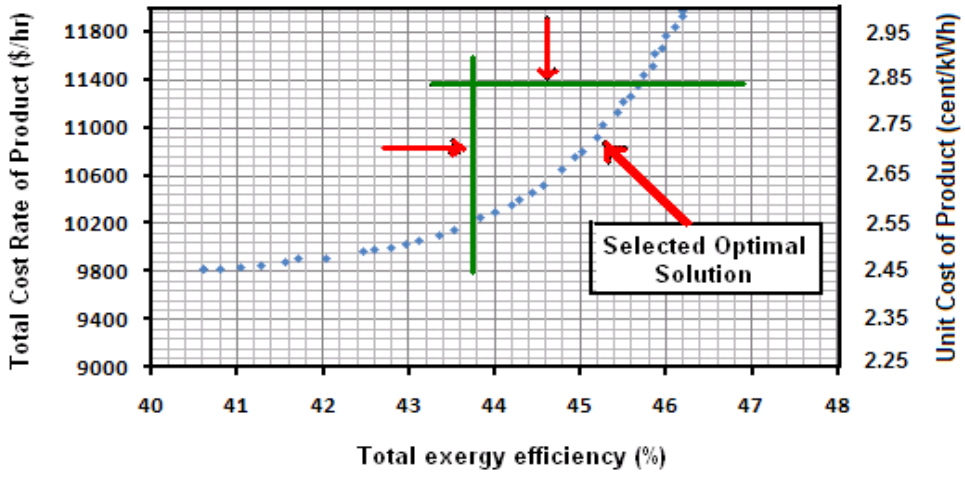

Fig. 6. Selecting procedure for optimal solution from Pareto frontier in the system shown in Fig. 3

The cost of the streams in the base case and optimum cases (single and multi objective optimization) are given in Table 6. Unit cost of the electricity produced by steam turbine is reduced from 29.57 cents/kWh in the base case to 27.47 and 27.63 cents/kWh in the optimum cases respectively.

The related values of decision variables in both optimum cases are given in Table 7. These new parameters obtained in the optimized cases will help the designer to select components, i.e. turbines, compressor, as close to the optimum configuration.

State points (Fig. 2)	Base case		Optimum case (Single objective)		Optimum case (Multi objective)	
	c (cents/kWh)	C ($/h)	c (cents/kWh)	C ($/h)	c (cents/kWh)	C ($/h)
1	0	0	0	0	0	0
2	24.44	32474	24.19	29873	24.24	30219
3	20.88	81093	20.64	74980	20.68	77156
4	20.88	22097	20.64	19069	20.68	21474
5	20.88	16758	20.64	13736	20.68	15675
6	20.88	6632	20.64	5670	20.68	6337
7	20.88	4301	20.64	3703	20.68	4091
8	20.88	4050	20.64	3477	20.68	3856
9	20.88	2480	20.64	2146	20.68	2337
10	20.88	1254	20.64	1103	20.68	1159
11	25.99	7343	25.30	6067	25.44	6798
12	25.99	209	25.30	176	25.44	198
13	31.49	346	29.06	275	30.27	321
14	34.77	1422	34.01	1200	34.45	1361
15	35.59	189	34.29	158	35.05	180
16	22.98	1799	22.22	1523	22.64	1736
17	25.07	2074	24.27	1769	24.61	1994
18	35.59	1564	34.29	1328	35.05	1517
19	30.07	3960	29.32	3352	29.94	3826
20	30.07	3075	29.32	2504	29.94	2879
21	24.99	13272	24.12	10629	24.70	12281
22	26.88	18383	26.61	15700	26.43	17465
23	26.07	23785	25.39	21089	25.51	23325
24	30.07	885	29.32	848	29.94	947
25	33.44	5111	33.97	5070	31.70	5184
26	22.92	8378	23.84	9226	21.78	10234
27	23.14	8526	24.02	9366	21.97	10399
28	22.92	16773	23.84	17613	21.78	18647
29	0	0	0	0	0	0
30	51.90	7145	50.52	5901	50.80	6611
31	12.09	48593	12.09	45077	12.09	46908
32	0	0	0	0	0	0
33	29.57	148	27.47	139	27.63	165
34	29.57	137	27.47	99	27.63	124
35	29.57	331	27.47	285	27.63	337
36	22.18	31760	21.92	28981	21.92	29754
37	22.18	59484	21.92	57012	21.92	56214
38	29.57	44384	27.47	39659	27.63	43850

Table 6. Cost of streams in the system shown in Fig. 3

Decision variables	Base case	Optimum case (Single objective)	Optimum case (Multi objective)
Compressor efficiency	85	85.98	82.98
Compressor pressure ratio	11	11.98	10.86
Inlet temperature of gas turbine (K)	1404.8	1449.9	1437.8
Gas turbine efficiency (%)	87.5	90	87.98
Oil outlet temperature (K)	666.5	658.17	650.28
Inlet pressure to HP steam turbine (bar)	84.8	99.91	96.24
Inlet temperature to HP steam turbine (K)	779.15	823.13	808.66
Inlet pressure to LP steam turbine (bar)	9.1	9.97	9.95
Steam turbine efficiency (%)	85	89.94	89.99
CEP efficiency (%)	80	88.84	80
BFP efficiency (%)	80	84.02	77.84
OILP efficiency (%)	80	83.44	86.16

Table 7. Comparison of the decisions variables for optimum and base cases in the system shown in Fig. 3

The values of objective functions in the base and optimum cases including the total cost of product and the total exergy efficiency are listed in Table 8. This table indicates that the optimization process leads to 10.98% decrease in the objective function for single objective optimization and 3.2% increase in the exergetic efficiency and 3.82% decrease for the rate of product cost in multi objective optimization. Therefore, improvement for all objectives has been achieved using optimization process.

The comparative results of the base case and the optimum cases are presented in Table 9. According to this table, optimization process improves the total performance of the system in a way that the rate of fuel cost is decreased by 7.23 and 3.46% in optimum cases. Also exergy destructions is reduced about 12 and 5.7%, the related cost of the system inefficiencies is decreased about 14.8 and 7.32% and exergetic efficiency is increased from 43.79 to 46.8 and 45.19% in both optimum cases, although the total owning and operation cost in single objective optimization is increased about 13.3%. Moreover, it can be found from this table that the optimization increases the overall exergoeconomic factor of this system from 12.18 in the base case to 15.51 (27.34% increases) and 12.56 (3.1% increase) implying that optimization process mostly reduced the associated cost of thermodynamic inefficiencies rather to increase the capital investment and operating and maintenance cost of the system components

Type of optimization	Objective functions	Base case	Optimum case	Variation (%)
Single objective optimization	Objective optimization ($/h)	93179.46	82942.52	-10.98
Multi object optimization	Total cost of product ($/h)	11354.02	10920.43	-3.82
	Total exergy efficiency (%)	43.79	45.19	+3.2

Table 8. Comparison of the objective functions for optimum and base cases in the system shown in Fig. 3

Properties	Base case	Single objective		Multi objective	
		Optimum case	Variation %	Optimum case	Variation %
Fuel exergy (solar+gas) (MW)	511.02	481.94	-5.69	497.07	-2.73
Exergy destruction (MW)	456.39	401.31	-12.07	430.31	-5.71
Fuel cost ($/h)	48593	45077	-7.23	46908	-3.46
Exergy destruction cost ($/h)	79255.75	67506.68	-14.82	73454.3	-7.32
Capital investment cost ($/h)	11354.02	12866.14	+13.31	10920.43	-3.82
Exergy efficiency (%)	43.79	46.80	+6.87	45.19	+3.2
Exergoeconomic factor (%)	12.18	15.51	+27.34	12.56	+3.1

Table 9. Comparative results of the optimum and base cases in the system shown in Fig. 3

10.4 Sensitivity analysis of the ISCCS

10.4.1 Sensitivity analysis for single objective optimization

Additional runs of the optimization algorithm were performed on the system in order to investigate the influence of the unit cost of fuel, the construction period and solar operation period on the solution. Fig. 7 shows sensitivity with respect to fuel cost which is linear. Fig. 8 illustrates variation of unit cost with increasing solar contribution which is significant (Baghernejad & Yaghoubi, 2011a).

10.4.2 Sensitivity analyses for multi objective optimization

Fig. 9 shows the sensitivity of the Pareto optimal Frontier to the variation of specific fuel cost. A comparison of the Pareto frontiers for the three optimizations shows that the economic minimum at higher unit costs of fuel is shifted upwards as expected. Similar behavior is observed for sensitivity of Pareto optimal solution to the construction period in Figures 10. In fact the exergetic objective has no sensitivity to the economic parameters such as the fuel cost and construction period (Baghernejad & Yaghoubi, 2011b).

The final optimal solution that was selected in this system belongs to the region of Pareto frontier with significant sensitivity to the costing parameters. However, the region with the lower sensitivity to the costing parameter is not reasonable for the final optimum solution. Also a small change in exergetic efficiency of the plant (exergetic efficiency from 47% to the higher value) due to the variation of operating parameters may lead to the danger of increasing the cost rate of product, drastically.

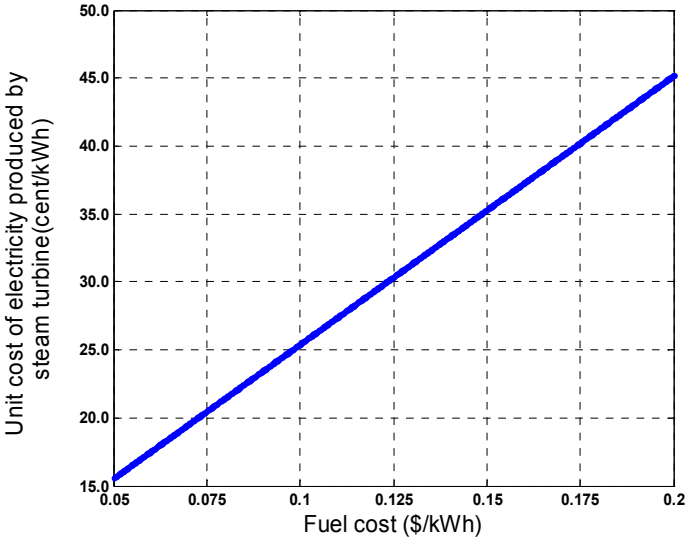

Fig. 7. Sensitivity of unit cost of electricity with specific fuel cost

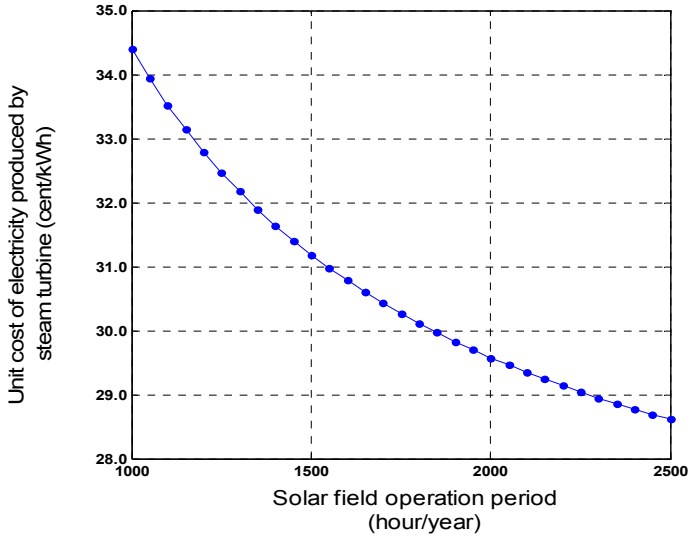

Fig. 8. Sensitivity of unit cost of electricity to the solar field operation periods

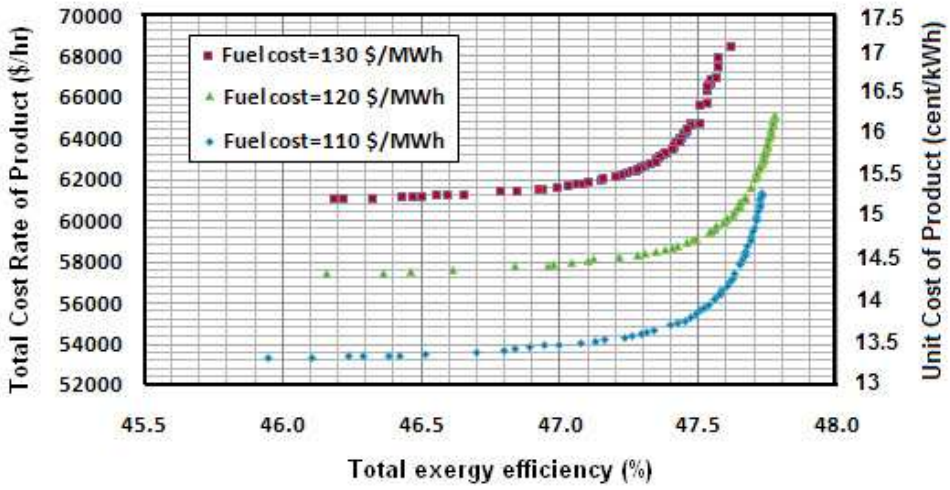

Fig. 9. Sensitivity of Pareto optimum solutions to the specific fuel cost

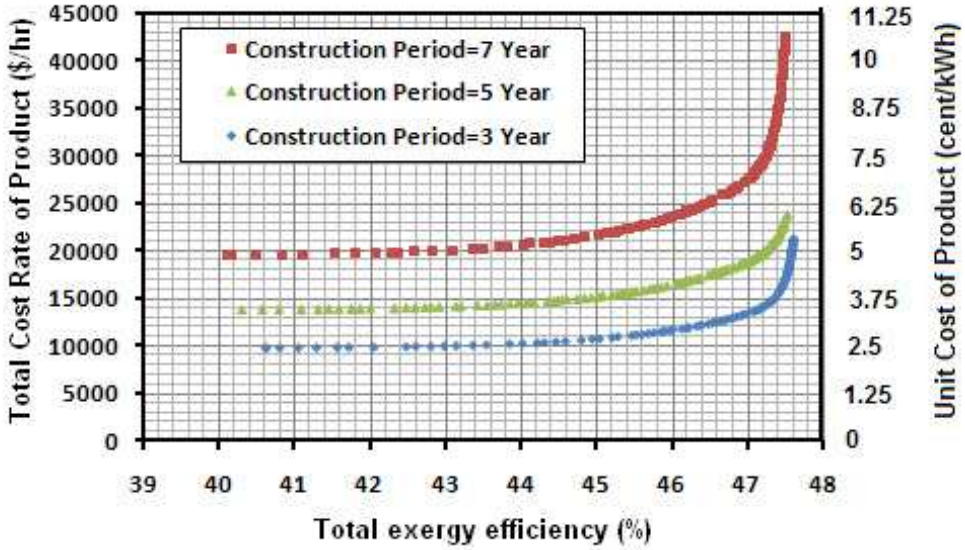

Fig. 10. Sensitivity of Pareto optimum solutions to the construction period

11. Conclusion

The presented chapter demonstrates the basic of exergoeconomic modeling of any thermal power plant and application of the exergoeconomic concept to single and multi objective optimization of an Integrated Solar Combined Cycle System (ISCCS). The exergy-costing method is applied to a 400 MW Integrated Solar Combined Cycle System to estimate the unit costs of electricity produced from combined gas and steam turbines.

The application of single objective optimization process shows that exergy and exergoeconomic analysis improved significantly for optimum operation as follows:

1. Objective function decreased by about 11% and overall exergoeconomic factor of system increased by 27.34 %.
2. Unit cost of electricity produced by steam turbine reduced by about 7.1%. This is achieved, however, with 13.3% increase in the capital investment.
3. Exergy destruction cost reduced by 14.82% and exergetic efficiency of the system increased from about 43.79 to 46.8%.

Also, it is found that multi-criteria optimization approach, which is a general form of single objective optimization, enables us to consider various and ever competitive objectives for more improvement of any thermal power plant. An example of decision-making process for selection of the final optimal solution from the Pareto frontier in the multi objective optimization is presented. This final optimum solution requires a process of decision-making, which depends on the preferences and criteria of each decision-maker. Each decision maker may select different points as optimum solution which better suits with their desires. The final optimum solution for a typical ISCCS is determined and compared to the base case design and discussed. The analysis of the ISCCS shows that:

1. Optimization process leads to 3.2% increase in the exergetic efficiency and 3.82% decrease of the rate of product cost.
2. Optimization leads to the 2.73% reduction on the fuel exergy, 5.71% reduction in the total exergy destruction and also 3.46% and 7.32% reductions in the fuel cost rate and cost rate relating to the exergy destruction, respectively.
3. It is found that multi-criteria optimization approach, which is a general form of single objective optimization, enables us to consider various and ever competitive objectives.

12. Nomenclature

AC	air compressor	P_r	pressure ratio
BFP	boiler feed pump	ri	rate of inflation
c	cost per exergy unit, $/kWh	s	specific entropy, kJ/kgK
$\dot{C}$	cost rate, $/h	SCA	solar collector assembly
CC	combustion chamber	SH	superheater
CEP	condensate extraction pump	SHE	solar heat exchanger
COLL	collector	ST	steam turbine
COND	condenser	T	temperature, K
CP	construction period, year	$\dot{W}$	power, MW
DEA	dearator	$\dot{Z}$	investment cost rate, $/h
$\dot{E}$	exergy rate, MW	Greek symbols	
ECO	economizer	ε	exergetic efficiency
EVA	evaporator	φ	maintenance factor
f	exergoeconomic factor/ annuity factor	η	isentropic efficiency
GT	gas turbine	χ	relative irreversibility
h	specific enthalpy, kJ/kg	ϕ	scaling factor
H	operation period, hour	σ	standard deviation
HCE	heat collection element	Subscripts	
HP	high pressure	1,2,3…,38	state points
HRSG	heat recovery steam generator	CH	chemical exergy
HTF	heat transfer fluid	D	destruction
I	equipment investment, $	e	outlet
in	interest rate	i	inlet/ith flow stream
k	plant lifetime, year	k	k^{th} component
LHV	lower heating value	L	loss
LP	low pressure	F	fuel
$\dot{m}$	mass flow rate, kg/sec	P	product
OILP	oil pump	PH	physical exergy
P	pressure, bar	sys	system
P'	offspring	tot	total

13. References

Baghernejad, A. Yaghoubi, M. (2010). Exergy Analysis of an Integrated Solar Combined Cycle System. *Renewable Energy*, Vol.35, No.10, pp. 2157-2164, ISSN 0960-1481

Baghernejad, A. Yaghoubi, M. (2011a). Exergoeconomic Analysis and Optimization of an Integrated Solar Combined Cycle System (ISCCS) Using Genetic Algorithm. *Energy conversion and Management,* Vol.52, No.5, pp. 2193-2203, ISSN 0196-8904

Baghernejad, A. Yaghoubi, M. (2011b). Multi objective exergoeconomic optimization of an integrated solar combined cycle system using evolutionary algorithms. *International Journal of Energy Research,* Vol.6, No.7, pp. 601-615

Bejan, A. Tsatsaronis, G & Moran, M. (1996). Thermal design and optimization, John Wiley and Sons, New York

Beghi, A. Cecchinato, L & Rampazo, M. (2011). A multi-phase genetic algorithm for the efficient management of multichiller systems, *Energy Conversion and Management.* Vol.52, No.3, pp. 1650-1661, ISSN 0196-8904

Cammarata, G. Fichera, A & Marletta, L. (1998). Using genetic algorithms and the exergonomic approach to optimize district heating networks, *ASME: Journal of Energy Resource Technology*, Vol.120, No.3, pp. 241–246

Concentrated solar thermal power-now. (2005). www.greenpeace.org. Sep. 2005.

Johansson, A. (2002). Entropy and the cost of complexity in industrial production. *Exergy an International Journal.* Vol.2, No.4, pp. 295–299.

Kearney, D. (1999). Parabolic-Trough Technology Roadmap A Pathway for Sustained Commercial Development and Deployment of Parabolic-Trough Technology. SunLab NREL.

Lazzaretto, A. Tsatsaronis, G. (2006). SPECO: a systematic and general methodology for calculating efficiencies and costs in thermal systems. *Energy*, Vol.31, No.8, pp. 1257–1289

Lazzaretto, A. Toffolo, A. (2004). On the thermoeconomic approach to the diagnosis of energy system malfunctions. Indicators to diagnose malfunctions: Application of a new indicator for the location of causes. *Int. J. Thermodynamics*, Vol.7, No.2, pp. 41–49.

Lozano, M. Valero, A. (1993). Theory of the exergetic cost. *Energy*, Vol.18, No.9, pp. 939–960.

Moran, M. Sciubba, E. (1994). Exergy analysis: principles and practice. *Gas Turbines Power,* Vol.116, No.2, pp. 285–290

Pareto V. (1896). Cours d'economie politique. Lausanne, Switzerland

Rao SS. (1996). Engineering optimization: theory and practice, John Wiley and Sons, New York

Rezende, M. Costa, C. Costa, A. Maciel, M & Filho, R. (2008). Optimization of a large scale industrial reactor by genetic algorithms. *Chemical Engineering Science*. Vol.63. No.2, pp. 330-341

Schwarzenbach, A. Wunsch, AK. (1989). Flexible power generation systems and their planning, ABB Review No.6, pp. 19-26

Schwefel HP. (1995). Evolution and optimum seeking, John Wiley and Sons, New York

Singh, N. Kaushik, SC. (1994). Technology assessment and economic evaluation of solar thermal power generation. IIT, Delhi: CES

Status Report on Solar Thermal Power Plants, Pilkington Solar International: 1996. Report ISBN 3-9804901-0-6.

Tsatsaronis, G. Pisa, J. (1994). Exergoeconomics evaluation and optimization of energy systems—application to the CGAM problem. *Energy*, Vol.19, No.3, pp. 287–321

Valero, A. Correas, L. Zaleta, A. Lazzaretto, A. Verda, V. Reini, M & Rangel, V. (2004). On the thermoeconomic approach to the diagnosis of energy system malfunctions. part 1: the tadeus problem. *Energy*, Vol.29, No.12-15, pp. 1875–1887.

Verda, V. (2004). Thermoeconomic analysis and diagnosis of energy utility systems. From diagnosis to prognosis. *Int. J. Thermodynamics*. Vol.7, No.2, pp. 73–83, ISSN 1301-9724

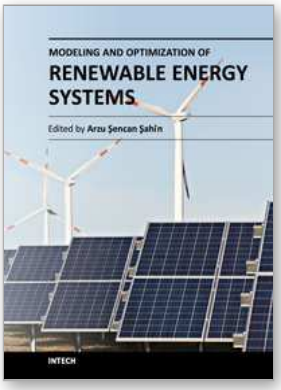

Modeling and Optimization of Renewable Energy Systems
Edited by Dr. Arzu Şencan

ISBN 978-953-51-0600-5
Hard cover, 298 pages
Publisher InTech
Published online 11, May, 2012
Published in print edition May, 2012

This book includes solar energy, wind energy, hybrid systems, biofuels, energy management and efficiency, optimization of renewable energy systems and much more. Subsequently, the book presents the physical and technical principles of promising ways of utilizing renewable energies. The authors provide the important data and parameter sets for the major possibilities of renewable energies utilization which allow an economic and environmental assessment. Such an assessment enables us to judge the chances and limits of the multiple options utilizing renewable energy sources. It will provide useful insights in the modeling and optimization of different renewable systems. The primary target audience for the book includes students, researchers, and people working on renewable energy systems.

How to reference
In order to correctly reference this scholarly work, feel free to copy and paste the following:

Ali Baghernejad and Mahmood Yaghoubi (2012). Exergoeconomic Analysis and Optimization of Solar Thermal Power Plants, Modeling and Optimization of Renewable Energy Systems, Dr. Arzu Şencan (Ed.), ISBN: 978-953-51-0600-5, InTech, Available from: http://www.intechopen.com/books/modeling-and-optimization-of-renewable-energy-systems/exergoeconomic-analysis-and-optimization-of-solar-thermal-power-plants

INTECH
open science | open minds

InTech Europe
University Campus STeP Ri
Slavka Krautzeka 83/A
51000 Rijeka, Croatia
Phone: +385 (51) 770 447
Fax: +385 (51) 686 166
www.intechopen.com

InTech China
Unit 405, Office Block, Hotel Equatorial Shanghai
No.65, Yan An Road (West), Shanghai, 200040, China
中国上海市延安西路65号上海国际贵都大饭店办公楼405单元
Phone: +86-21-62489820
Fax: +86-21-62489821